Inorganic Chemistry

including bioinorganic chemistry

April 21, 2014
Volume 53, Number 8
pubs.acs.org/IC

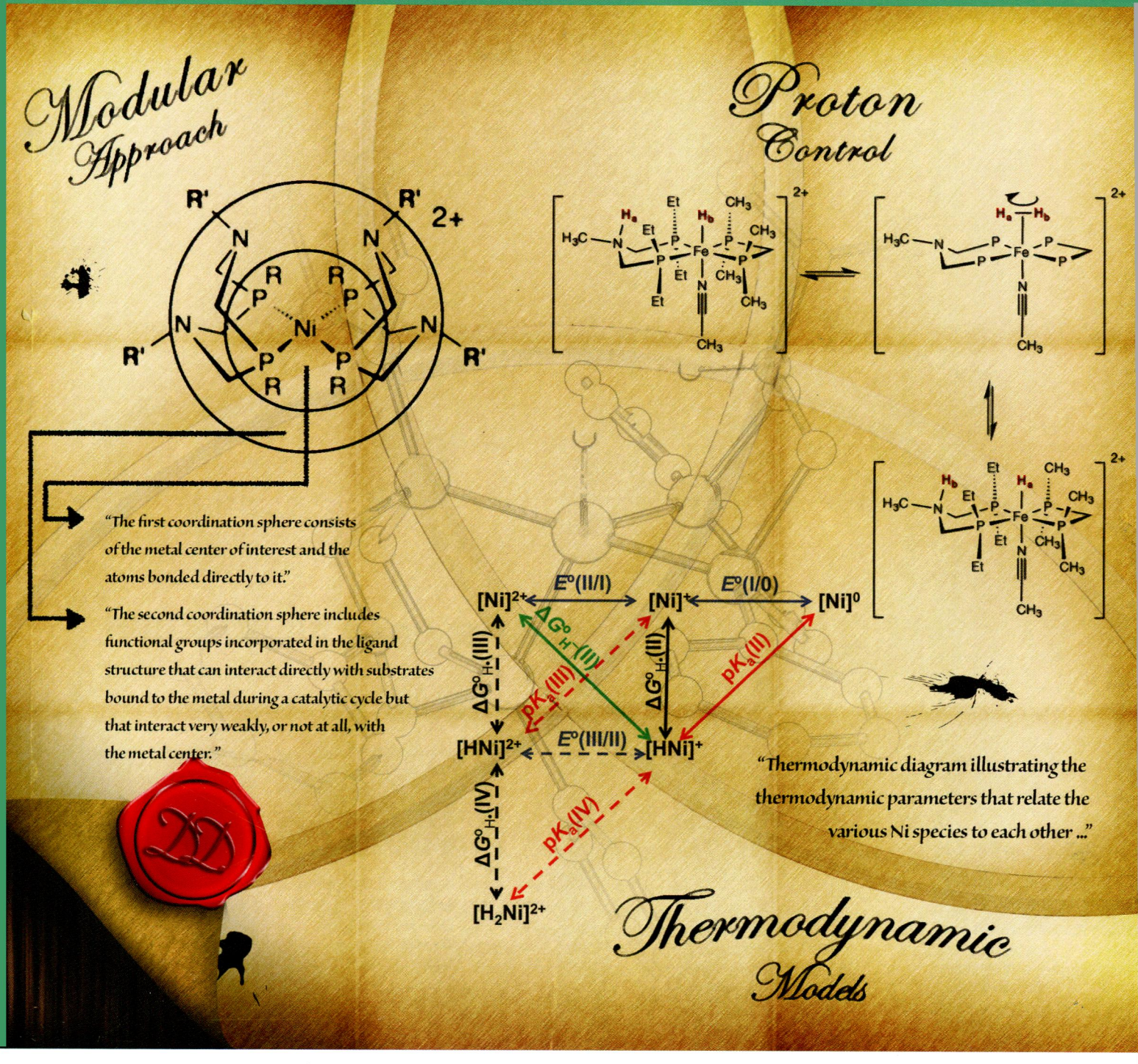

Inorganic Chemistry

APRIL 21, 2014
VOLUME 53 ISSUE 8
INOCAJ 53(8) 3921−4268 (2014)
ISSN 0020-1669
Registered in the U.S. Patent and Trademark Office

ON THE COVER: Proton relays, thermodynamic models, and the conceptual partitioning of catalysts into coordination spheres are important themes in the design of molecular electrocatalysts for energy storage. See the Award Article by D. L. DuBois, p 3935. Cover design by Jonathan M. Darmon.

Editorial

3921 dx.doi.org/10.1021/ic500707b

Editorial for the Virtual Issue on Inorganic Cages and Containers
Alan L. Balch

Communications

3926 dx.doi.org/10.1021/ic4030316

Two Isostructural 3D Lanthanide Coordination Networks (Ln = Gd^{3+}, Dy^{3+}) with Squashed Cuboid-Type Nanoscopic Cages Showing Significant Cryogenic Magnetic Refrigeration and Slow Magnetic Relaxation
Soumava Biswas, Himanshu Sekhar Jena, Amit Adhikary, and Sanjit Konar*

Two isostructural lanthanide-based 3D coordination networks [Ln = Gd^{3+} (**1**), Dy^{3+}(**2**)] with densely packed distorted cuboid nanoscopic cages are reported. Magnetic characterization reveals that complex **1** shows a significant cryogenic magnetocaloric effect ($-\Delta S_m$ = 44.0 J kg^{-1} K^{-1}), whereas **2** shows slow relaxation of magnetization.

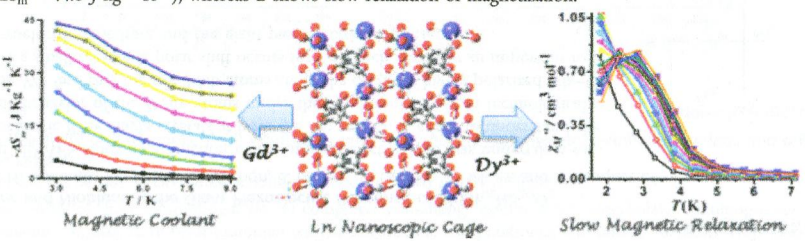

3929 dx.doi.org/10.1021/ic500360f

Cisplatin Binding to Proteins: Molecular Structure of the Ribonuclease A Adduct
Luigi Messori and Antonello Merlino*

The crystal structure of the main adduct formed in the reaction between cisplatin and bovine pancreatic ribonuclease is reported here. Notably, in both of the protein molecules present in the asymmetric unit, platinum(II) binding takes place exclusively at the level of Met29. In one of the two molecules, the Gln28 side chain completes the platinum coordination sphere, anchoring the cisplatin fragment to the protein in a bidentate fashion. These results contain interesting implications for understanding the biological chemistry of this important drug.

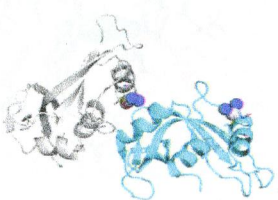

3932 Ⓢ dx.doi.org/10.1021/ic500562r

Synthesis and Structure Determination of a New Au_{20} Nanocluster Protected by Tripodal Tetraphosphine Ligands
Jing Chen, Qian-Fan Zhang, Paul G. Williard, and Lai-Sheng Wang*

A new Au_{20} nanocluster, coordinated by four tripodal tetraphosphine ligands, has been synthesized and crystallized. The Au_{20} core is chiral and consists of an icosahedral Au_{13} cluster core and a seven-Au-atom partial outer shell arranged in a tripodal shape with local C_3 symmetry.

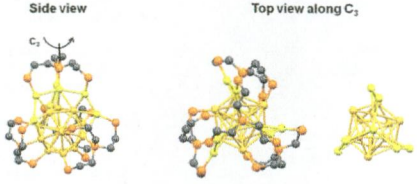

Award Paper

3935 dx.doi.org/10.1021/ic4026969

Development of Molecular Electrocatalysts for Energy Storage
Daniel L. DuBois

The development of molecular electrocatalysts for energy conversion reactions includes the proper design of first, second, and outer coordination spheres, proton relays to control the proton movement between coordination spheres, and energy matching within and between coordination spheres.

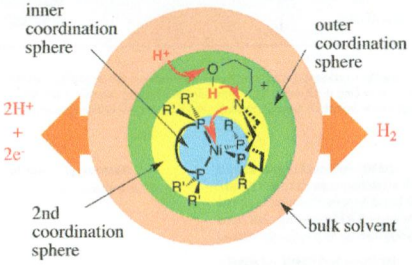

Articles

3961 Ⓢ dx.doi.org/10.1021/ic500279q

Defects in Chemically Synthesized and Thermally Processed ZnO Nanorods: Implications for Active Layer Properties in Dye-Sensitized Solar Cells
Partha Pratim Das, Shruti A. Agarkar, Soumita Mukhopadhyay, Unnikrishnan Manju, Satishchandra B. Ogale, and P. Sujatha Devi*

We have carried out the effect of post annealing temperatures on the DSSC performance of solution-grown ZnO rods prepared by a modified sonochemical process. We could conclude that the ZnO rods exhibiting minimum native defects and highest excitonic emission, that is, rods annealed at 300 °C, are better suited for fabricating DSSC with improved efficiency (1.57%), current density (5.11), and fill factor (45.29%).

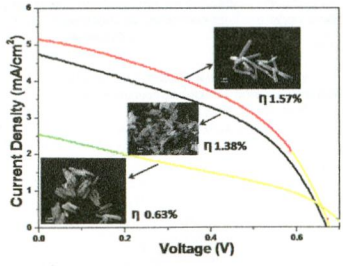

3973 S dx.doi.org/10.1021/ic402340d

Water Oxidation Chemistry of a Synthetic Dinuclear Ruthenium Complex Containing Redox-Active Quinone Ligands

Hiroshi Isobe,* Koji Tanaka, Jian-Ren Shen, and Kizashi Yamaguchi

Water oxidation by a dinuclear ruthenium complex has been investigated theoretically. The ability of redox-active quinone ligands to store redox equivalents leads to an electronic flexibility of the catalyst that causes water activation to be thermodynamically and kinetically favorable. On the other hand, the catalyst binds a μ-peroxo ligand too strongly to release O_2, unless a large hinge-like bending motion permits the catalyst to open its reaction site for incorporating a substrate water molecule.

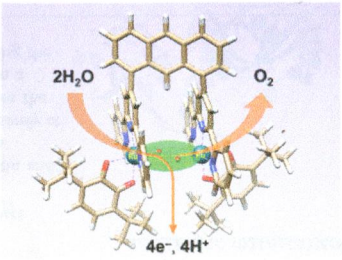

3985 dx.doi.org/10.1021/ic402409f

Role of Zinc and Niobium in the Giant Piezoelectric Response of $PbZn_{1/3}Nb_{2/3}O_3$

A. Al-Zein, H. Dammak, Ph. Papet, O. Mathon, B. Hehlen, C. Levelut, J. Haines, and J. Rouquette*

An "in situ" EXAFS study as a function of the applied electric field was undertaken on giant piezoelectric PZN single crystals at both the Nb and Zn *K* edges to understand the atomic-scale behavior of the *B*-site atoms under the conditions of use in technological applications. We find that the small Nb atoms are at the origin of highly polarized Nb−O bonds while a small reversible polar shift occurs for Zn which may play an important role in both ferroelectric switching and the giant piezoelectric response.

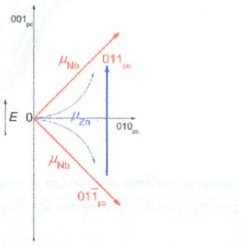

Simplified scheme of the B-site behaviour under electric field in the PZN poled sample.

3991 S dx.doi.org/10.1021/ic4028223

Syntheses of a Novel Fluorinated Trisphosphinoborate Ligand and Its Copper and Silver Complexes. Catalytic Activity toward Nitrene Transfer Reactions

Ismael Arenas, M. Ángeles Fuentes, Eleuterio Álvarez, Yolanda Díaz,* Ana Caballero,* Sergio Castillón,* and Pedro J. Pérez*

A novel trisphosphinoborate ligand containing fluorinated groups in the aryl ring bonded to the P donors has been synthesized. Its coordination to copper and silver ions has provided new complexes with catalytic capabilities toward nitrene transfer reactions that improve those of the parent unsubstituted ligand. The effect seems to be purely electronic, given that structural parameters have not substantially changed upon incorporation of the CF_3 groups.

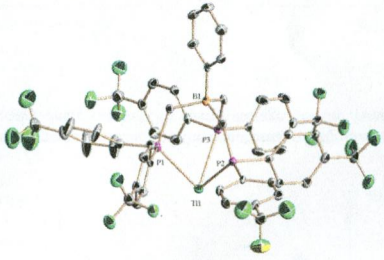

4000 (S) dx.doi.org/10.1021/ic402890k

A Convenient Route to Synthetic Analogues of the Oxidized Form of High-Potential Iron–Sulfur Proteins

Kazuki Tanifuji, Norihiro Yamada, Tomoyuki Tajima, Takahiro Sasamori, Norihiro Tokitoh, Tsukasa Matsuo, Kohei Tamao, Yasuhiro Ohki, and Kazuyuki Tatsumi*

An amide-bound $[Fe_4S_4]^{3+}$ cluster, $[Fe_4S_4\{N(SiMe_3)_2\}_4]^-$ (**1**), was found to serve as a convenient precursor for synthetic analogues of the oxidized form of high-potential iron–sulfur proteins. Treatment of **1** with 4 equiv of bulky thiols led to the formation of $[Fe_4S_4(SR)_4]^-$ (R = bulky substituents). The electrochemical properties of these $[Fe_4S_4]^{3+}$ clusters are discussed.

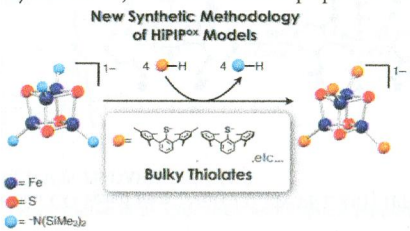

4010 (S) dx.doi.org/10.1021/ic402909t

Removal of Selenite from Water Using a Synthetic Dithiolate: An Experimental and Quantum Chemical Investigation

Daniel Burriss, Wenli Zou, Dieter Cremer,* John Walrod, and David Atwood*

Computational analyses and ^{77}Se NMR demonstrate that the dithiol $BDTH_2$ combines with H_2SeO_3 (selenite) to form a two-coordinate Se(II) compound with a S–Se–S linkage. The compound is highly susceptible to reductive decomposition to form red Se(0) and the dithiolate BDT(S–S).

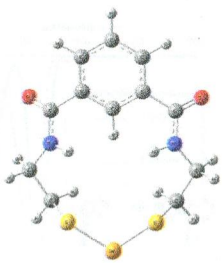

4022 (S) dx.doi.org/10.1021/ic402980t

Solid-State Electrochemistry of a Semiconducting MMX-Type Diplatinum Iodide Chain Complex

Hiroaki Iguchi,* Ayman Nafady, Shinya Takaishi, Masahiro Yamashita, and Alan M. Bond*

The solid-state electrochemical behavior of the semiconducting MMX-type diplatinum-iodide chain complex has been investigated by cyclic voltammetry. Chemical reversibility is evident in the oxidation process, and the reduction peak potentials depend on the electrolyte cation size. The presence of acid (H^+) induces product dissolution on repetitive cycling of the potential. The results provide a platform for developing electrochemical devices based on this type of semiconducting porous coordination compound.

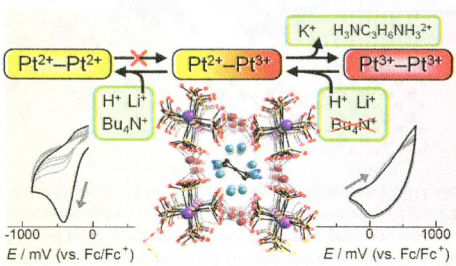

4029 S dx.doi.org/10.1021/ic4030475

A Ditopic O_4S_2 Macrocycle and Its Hard, Soft, and Hard/Soft Metal Complexes Exhibiting Endo-, Exo-, or Endo/Exocyclic Coordination: Synthesis, Crystal Structures, NMR Titration, and Physical Properties

Hyunsoo Ryu, Ki-Min Park, Mari Ikeda, Yoichi Habata, and Shim Sung Lee*

The proposed O_4S_2 macrocycle enabled us to prepare several supramolecular complexes with different structural types and coordination modes, including a heteronuclear [Na(I)/Cu(I)] 2D coordination network with the endo- and the exocyclic coordination modes simultaneously.

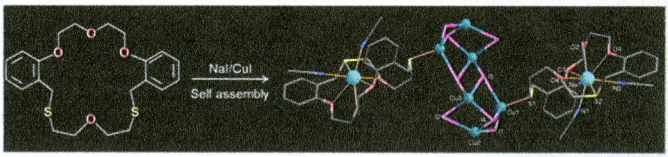

4039 S dx.doi.org/10.1021/ic403069d

Guest-Effected Spin-Crossover in a Novel Three-Dimensional Self-Penetrating Coordination Polymer with Permanent Porosity

Jin-Yan Li, Zheng Yan, Zhao-Ping Ni,* Ze-Min Zhang, Yan-Cong Chen, Wei Liu, and Ming-Liang Tong*

A new 3D self-penetrated network with in-situ-generated $[Ag_2(CN)_3]^-$ motifs displays two-step guest-effected SCO with hysteresis and permanent porosity (299 $Å^3$ per iron atom) after desolvation, which is one of the largest volume values of porosity for the Hoffman-like SCO coordination polymers to date.

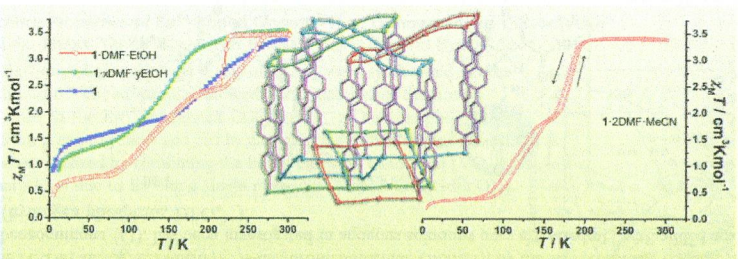

4047 S dx.doi.org/10.1021/ic403126p

Dioxygen Reactivity of Biomimetic Fe(II) Complexes with Noninnocent Catecholate, *o*-Aminophenolate, and *o*-Phenylenediamine Ligands

Michael M. Bittner, Sergey V. Lindeman, Codrina V. Popescu,* and Adam T. Fiedler*

The O_2 reactivities of three mononuclear Fe(II) complexes containing "noninnocent" catecholate, *o*-aminophenolate, and *o*-phenylenediamine ligands have been examined with spectroscopic, computational, and kinetic methods. Depending on the identity of the bidentate ligand, the O_2 reaction triggers iron-based oxidation, ligand-based oxidation, or a combination of both processes. The ligands are capable of donating protons as well as electrons, and the interplay between these two factors influences rates of reaction with O_2.

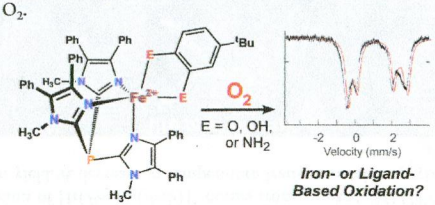

4062 dx.doi.org/10.1021/ic403163d

The Crystal and Electronic Structures of Cd_3As_2, the Three-Dimensional Electronic Analogue of Graphene

Mazhar N. Ali,* Quinn Gibson, Sangjun Jeon, Brian B. Zhou, Ali Yazdani, and R. J. Cava*

The structure of Cd_3As_2, a high-mobility semimetal reported to host electrons acting as Dirac particles, is reinvestigated by single-crystal X-ray diffraction and found to be centrosymmetric, correcting previous reports. It has a distorted superstructure of the antifluorite structure type with a tetragonal unit cell in the centrosymmetric $I4_1/acd$ space group. Electronic structure calculations imply that Cd_3As_2 is a 3D-Dirac semimetal with no spin splitting and a 3D electronic analogue of graphene.

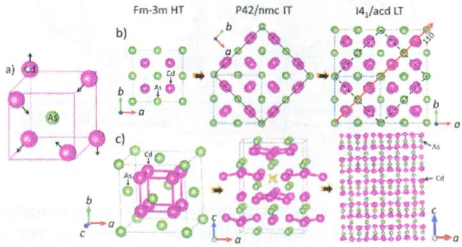

4068 dx.doi.org/10.1021/ic500022a

Structure–Activity Relationships in Cytotoxic Au^I/Au^{III} Complexes Derived from 2-(2′-Pyridyl)benzimidazole

Laura Maiore, Maria Carla Aragoni, Carlo Deiana, Maria Agostina Cinellu, Francesco Isaia, Vito Lippolis, Anna Pintus, Maria Serratrice, and Massimiliano Arca*

The electronic structure of 10 neutral and cationic mono- and dinuclear Au^I/Au^{III} complexes derived from 2-(2′-pyridyl)benzimidazole (pbiH), showing antitumor properties, was investigated on the basis of a combined electrochemical and spectroscopic approach paralleled by IEF-SCRF TD-DFT calculations in order to rationalize the cytotoxic activity against human ovarian carcinoma cell lines.

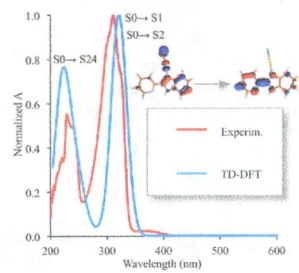

4081 dx.doi.org/10.1021/ic500025k

Thermal and Photochemical Reactivity of Manganese Tricarbonyl and Tetracarbonyl Complexes with a Bulky Diazabutadiene Ligand

Veeranna Yempally, Samuel J. Kyran, Rajesh K. Raju, Wai Yip Fan, Edward N. Brothers, Donald J. Darensbourg,* and Ashfaq A. Bengali*

Facile thermal substitution at 288 K of a CO ligand from $[Mn(CO)_4(^iPr_2Ph\text{-}DAB)]$ $[PF_6]$ (**2**) by acetonitrile to form the tricarbonyl complex $[Mn(CO)_3(CH_3CN)(^iPr_2Ph\text{-}DAB)]$ $[PF_6]$ (**3a**).

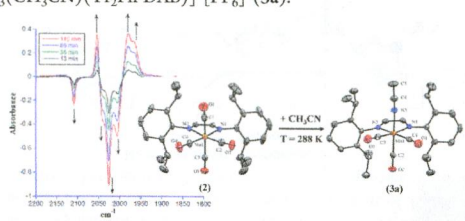

4089 Ⓢ dx.doi.org/10.1021/ic500070s

Blue-Green Iridium(III) Emitter and Comprehensive Photophysical Elucidation of Heteroleptic Cyclometalated Iridium(III) Complexes

Kassio P. S. Zanoni, Bruna K. Kariyazaki, Akitaka Ito, M. Kyle Brennaman, Thomas J. Meyer, and Neyde Y. Murakami Iha*

A complete photophysical investigation of a series of Ir(III) complexes by TD-DFT and Franck–Condon emission band shape analyses revealed that emission of $[Ir(Fppy)_2(dmb)]^+$ occurs from a mixed ^{3}MLCT/^{3}LC character excited state, which contributes to an unitary quantum yield. A decrease in temperature leads to notable spectral changes due to inversion in the lowest-lying excited state.

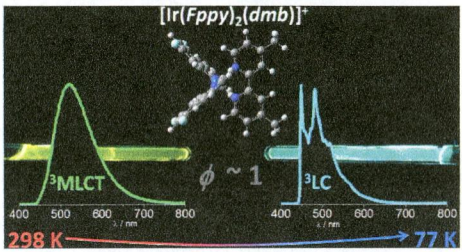

4100 Ⓢ dx.doi.org/10.1021/ic500072e

Multiple Pathways in the Oxidation of a NADH Analogue

Na Song, Ming-Tian Zhang, Robert A. Binstead, Zhen Fang, and Thomas J. Meyer*

Oxidation of the NADH analogue, *N*-benzyl-1,4-dihydronicotinamide (BNAH), by the $1e^-$ acceptor, $[Os(dmb)_3]^{3+}$, and $2e^-/2H^+$ acceptor, benzoquinone (Q), has been investigated in aqueous solutions over extended pH with added acid (acetic acid, HAc) or base (hydrogen phosphate, HPO_4^{2-}).

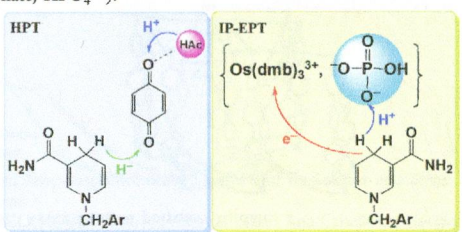

4106 dx.doi.org/10.1021/ic500090g

Synthesis and Characterization of $CuAlO_2$ and $AgAlO_2$ Delafossite Oxides through Low-Temperature Hydrothermal Methods

Dehua Xiong, Xianwei Zeng, Wenjun Zhang, Huan Wang, Xiujian Zhao, Wei Chen,* and Yi-Bing Cheng

The hydrothermal synthesis of submicrometer particulate $CuAlO_2$ and $AgAlO_2$ delafossite oxides, which are two important optically transparent and thermally stable *p*-type semiconducting oxides, have been systematically studied. The parameters that affect the crystal formation processes and the product morphologies, including the selection of starting materials and their molar ratios, the pH value of precursors, the hydrothermal temperature, pressure, and reaction time, have been investigated. The embedded crystal growth mechanisms have been uncovered.

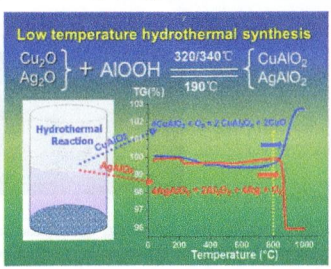

4117 dx.doi.org/10.1021/ic5000974

Single-Step Substitution of all the α, β-Positions in Pyrrole: Choice of Binuclear versus Multinuclear Complex of the Novel Polydentate Ligand

Debasish Ghorai and Ganesan Mani*

A new synthetic route for the $\alpha\alpha'\beta\beta'$-position-substituted pyrrole has been developed. The nuclearity of the metal complex of this polydentate ligand depends on which form is used—neutral or anionic.

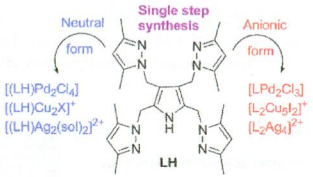

4130 dx.doi.org/10.1021/ic5001232

Tuning of Valence States, Bonding Types, Hierarchical Structures, and Physical Properties in Copper/Halide/Isonicotinate System

Min-Min Liu, Juan-Juan Hou, Zhi-kai Qi, Li–Na Duan, Wen-Juan Ji, Cai-yun Han, and Xian-Ming Zhang*

Hydrotherm treatment of cupric halide and isonicotinic acid generated seven cupric halide coordination polymers, one cupric complex templated cuprous halide, and one organic templated cuprous halide, as a consequence of the low standard electrode potential of Cu(II)/Cu(I) couple. Both normal X–Cu and weak X···Cu bonds were observed due to dynamic Jahn–Teller distortion of Cu(II) ions.

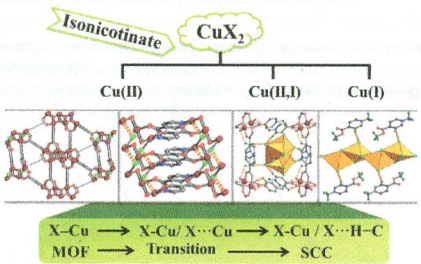

4144 dx.doi.org/10.1021/ic500163c

A Tripodal Benzylene-Linked Trisamidophosphine Ligand Scaffold: Synthesis and Coordination Chemistry with Group(IV) Metals

Sonja Batke, Malte Sietzen, Hubert Wadepohl, and Joachim Ballmann*

The synthesis of a tetradentate trisamidophosphine ligand is presented, and its coordination chemistry with group(IV) metals is described. A CH-activated titanium species and the ligand's tris-lithium salt are reported in addition to seven trigonal-bipyramidal $[PN_3]MX$ complexes (M = Ti, Zr, Hf; X = NMe_2, OTf, Cl).

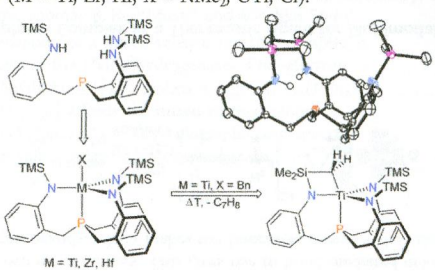

4154 (S) dx.doi.org/10.1021/ic500203k

Structures and Physical Properties of Layered Oxyselenides $Ba_2MO_2Ag_2Se_2$ (M = Co, Mn)

Tingting Zhou, Yumei Wang, Shifeng Jin,* Dandan Li, Xiaofang Lai, Tianping Ying, Han Zhang, Shijie Shen, Wenjun Wang, and Xiaolong Chen*

Two new layered oxyselenides, $Ba_2MO_2Ag_2Se_2$ (M = Co, Mn), have been successfully synthesized. Although the coexistence of a large barium ion and a Ag_2Se_2 layer expands the oxide layer significantly, the two title compounds both adopt an energetically more favorable $Sr_2Mn_3Sb_2O_2$-type structure, different from the *Cmca* model adopted by the zinc compound with discrete $[ZnO_2]^{2-}$ linear anionic units. Meanwhile, the magnetic, electronic-transport, and optical properties and structural variation tendency of these compounds are also investigated.

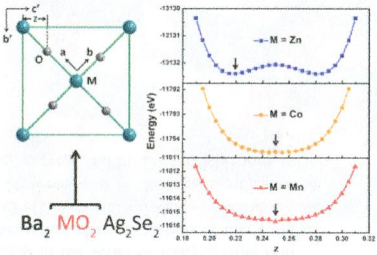

4161 dx.doi.org/10.1021/ic500208h

Photoluminescence Properties of Eu^{3+}-Doped Glaserite-Type Orthovanadates $CsK_2Gd[VO_4]_2$

Zhengxu Tao, Taiju Tsuboi, Yanlin Huang, Wei Huang, Peiqing Cai, and Hyo Jin Seo*

Undoped and Eu^{3+}-doped glaserite-type $CsK_2Gd[VO_4]_2$ were synthesized via the solid-state reaction. Eu^{3+}-doped samples showed nonquenching of the host emission even when in the Eu^{3+}-condensed $CsK_2Eu(VO_4)$. This phosphor shows tunable colors from green to yellow and red by changing the excitation wavelength. The white color was realized by combining the broad emission band from $[VO_4]^{3-}$ with intense sharp lines due to Eu^{3+} in a single phase Eu^{3+}-doped $CsK_2Gd[VO_4]_2$.

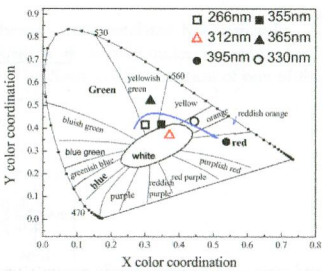

4169 (S) dx.doi.org/10.1021/ic500220d

Incorporation of Cu^{2+} Ions into Nanotubular Uranyl Diphosphonates

Pius O. Adelani, Nathaniel D. Cook, Jean-Marie Babo, and Peter C. Burns*

Three new multidimensional polymetallic uranyl diphosphonates have been synthesized under mild hydrothermal conditions and characterized via single-crystal X-ray diffraction. This is the first report on polymetallic uranyl diphosphonates to be constructed with bipym. The bipym group stabilizes the Cu(II) ions without truncating the dimensionality of the structure.

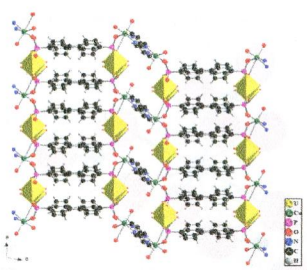

4177 dx.doi.org/10.1021/ic500221n

How Does Nishibayashi's Molybdenum Complex Catalyze Dinitrogen Reduction to Ammonia?

Yong-Hui Tian, Aaron W. Pierpont, and Enrique R. Batista*

In Nishibayashi's dinitrogen-reducing system, the dimolybdenum–dinitrogen complex is featured by a bimetallic structure, in which a dinitrogen bond bridges two metal centers. This gives rise to bond-mediated delocalized electronic states facilitating protonation of the apical dinitrogen ligands, which makes the bimetallic complex the effective catalyst instead of the monometallic fragment.

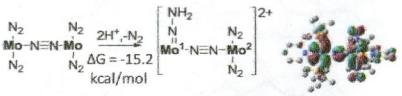

4184 dx.doi.org/10.1021/ic500238s

Tetranuclear Gadolinium(III) Porphyrin Complex as a Theranostic Agent for Multimodal Imaging and Photodynamic Therapy

Jian Luo, Li-Feng Chen, Ping Hu, and Zhong-Ning Chen*

Far-red-emitting high relaxivity with 107% increase upon binding to HSA together with efficiently generating singlet oxygen suggest Gd_4 complex as an excellent theranostic agent for MRI/optical imaging and photodynamic therapy.

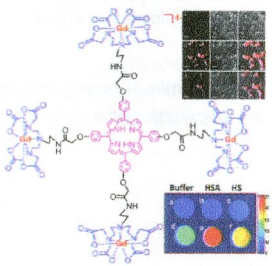

4192 dx.doi.org/10.1021/ic500311y

Synthesis, Structural Characterization, Reactivity, and Catalytic Properties of Copper(I) Complexes with a Series of Tetradentate Tripodal Tris(pyrazolylmethyl)amine Ligands

Estela Haldón, Manuela Delgado-Rebollo, Auxiliadora Prieto, Eleuterio Álvarez, Celia Maya, M. Carmen Nicasio,* and Pedro J. Pérez*

A series of cationic and neutral copper(I) complexes with tris(pyrazolylmethyl)-amine ligands (Tpa^x) have been prepared and characterized. The structures in the solid state reveal their polynuclear nature and a μ^2:κ^2:κ^1-coordination mode for the Tpa^x ligands, whereas NMR studies agree with the existence of fluxional behavior in solution.

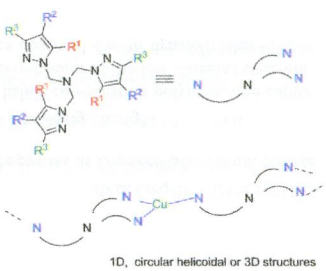

4202 dx.doi.org/10.1021/ic500314v

Kinetic Studies of the $[NpO_2(CO_3)_3]^{4-}$ Ion at Alkaline Conditions Using ^{13}C NMR

Adele F. Panasci, Stephen J. Harley, Mavrik Zavarin, and William H. Casey*

The kinetics of carbonate exchange on the $[NpO_2(CO_3)_3]^{4-}$ complex, shown here in ball-and-stick form, were measured as a function of solution pH. Reactivities compare well to the $[UO_2(CO_3)_3]^{4-}$ complex, which greatly simplifies geochemical predictions.

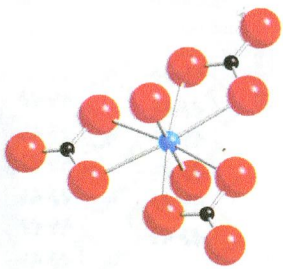

4209 dx.doi.org/10.1021/ic5003226

Highly Selective Sorption of Small Hydrocarbons and Photocatalytic Properties of Three Metal–Organic Frameworks Based on Tris(4-(1*H*-imidazol-1-yl)phenyl)amine Ligand

Hong-Ru Fu, Yao Kang, and Jian Zhang*

Presented here are three new metal–organic frameworks based on a tri(4-pyridylphenyl)amine ligand, showing photocatalytic properties and highly selective sorption of light hydrocarbons.

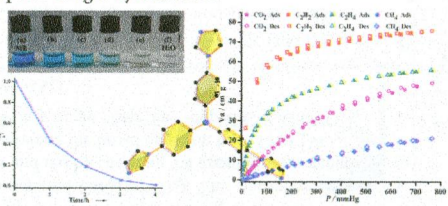

4215 dx.doi.org/10.1021/ic5003572

Phenyl Derivative of Iron 5,10,15-Tritolylcorrole

Sara Nardis, Daniel O. Cicero, Silvia Licoccia, Giuseppe Pomarico, Beatrice Berionni Berna, Marco Sette, Giampaolo Ricciardi, Angela Rosa,* Frank R. Fronczek, Kevin M. Smith,* and Roberto Paolesse*

The preparation of complex **1** fills a gap in the series of triarylcorrole iron derivatives. The spectroscopic and theoretical characterization of this complex indicates that it can be described as an Fe(IV) derivative, with a nonoxidized corrole species, acting as a trianionic ligand. However also in this case significant spin density is present on the corrole ring, as predicted by DFT calculations and confirmed by the ^1H NMR isotropic shifts.

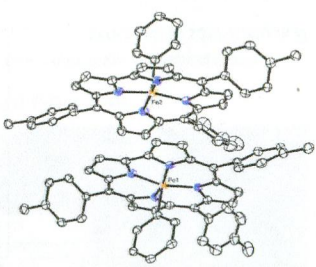

4228 dx.doi.org/10.1021/ic500367y

Synthesis, Crystal Structure, and Photoluminescence Studies of a Ruthenocenyl-Decorated Sn/S Cluster

Eliza Leusmann, Mona Wagner, Nils W. Rosemann, Sangam Chatterjee, and Stefanie Dehnen*

Upon an improved synthesis of acetylruthenocene (**1**) and the conversion of **1** to the corresponding hydrazone derivative, the reaction with keto-functionalized Sn/S complex $[(R^1Sn)_4S_6]$ (R^1 = CMe_2CH_2COMe) resulted in the formation of the first ruthenocene-decorated tin sulfide cluster $[(R^{Ru}Sn)_4Sn_2S_{10}]$ (**2**; R^{Rc} = $CMe_2CH_2C(Me)$=N–N=$C(Me)Rc$). We present the crystal structures of both **1** and **2** as well as the electrochemical behavior of **2** and its investigation by time-resolved photoluminescence (TRPL) studies.

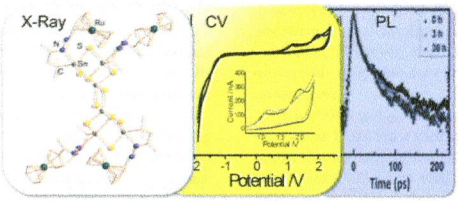

4234 dx.doi.org/10.1021/ic500375v

Hafnium Sulfate Prenucleation Clusters and the Hf_{18} Polyoxometalate Red Herring

Rose E. Ruther, Brenna M. Baker, Jung-Ho Son, William H. Casey, and May Nyman*

Aqueous Hf sulfate–peroxide solutions, "green" precursors for lithographically patterned thin films, exhibit complex behavior, forming polynuclear clusters and ultimately crystallizing the Hf_{18} polyoxometalate. Its ready formation has led to speculation of its existence in solution. Here, small-angle X-ray scattering and mass spectrometry probe solution evolution with time. Surprisingly, linked Hf tetramers and pentamers dominate the solution state, suggesting Hf_{18} is not an important species in kinetically precipitated gels that are precursors to thin-film materials.

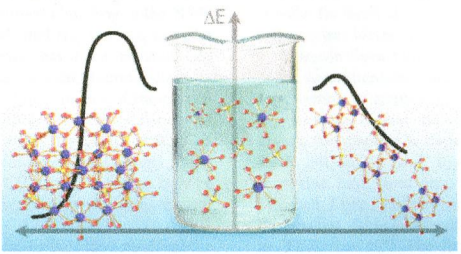

4243 dx.doi.org/10.1021/ic500389p

Ni^I/Ru^{II} Model for the Ni–L State of the [NiFe]Hydrogenases: Synthesis, Spectroscopy, and Reactivity

Geoffrey M. Chambers, Joyee Mitra, Thomas B. Rauchfuss,* and Matthias Stein*

This study describes the characterization of a mixed-valence Ru^{II}/Ni^I complex, a structural model for the Ni–L state of the [NiFe]hydrogenases. One-electron oxidation of (cymene)Ru(μ-pdt)Ni(diphos) ($[\mathbf{1}]^0$, diphos = dppe, $C_2H_4(PPh_2)_2$; $[\mathbf{2}]^0$, diphos = dcpe, $C_2H_4(P(C_6H_{11})_2)_2$] affords the mixed-valence cations $[(cymene)Ru(pdt)Ni(diphos)]^+$ ($[\mathbf{1}]^+$ and $[\mathbf{2}]^+$). Crystallographic and spectroscopic measurements indicate that these cations are described as Ru^{II}/Ni^I.

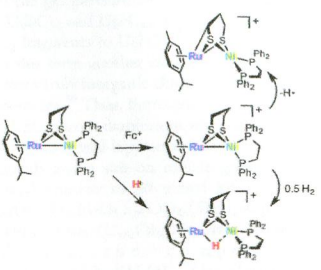

4250 dx.doi.org/10.1021/ic5003995

Crystal Structure and Magnetic Properties of $FeSeO_3F$—Alternating Antiferromagnetic $S = 5/2$ chains

Shichao Hu, Mats Johnsson,* Joseph M. Law, Jerry L. Bettis Jr., Myung-Hwan Whangbo, and Reinhard K. Kremer

The new oxofluoride $FeSeO_3F$ crystallizes in the space group $P2_1/n$ and consists of $[FeO_3F]_\infty$ zigzag chains with alternating Fe−F−Fe and Fe−O−Fe spin exchange paths. The magnetic susceptibility of $FeSeO_3F$ is largely described by an $S = 5/2$ Heisenberg antiferromagnetic chain with alternating antiferromagnetic spin exchanges, and $FeSeO_3F$ undergoes a long-range antiferromagnetic ordering below 45 K.

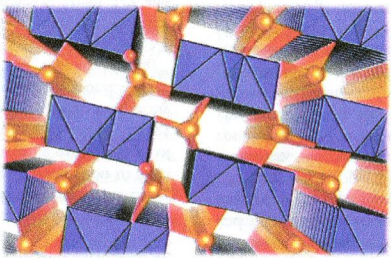

4257 dx.doi.org/10.1021/ic500705t

Reactivity of Coordinatively Unsaturated Bis(N-heterocyclic carbene) Pt(II) Complexes toward H_2. Crystal Structure of a 14-Electron Pt(II) Hydride Complex

Orestes Rivada-Wheelaghan, Marta Roselló-Merino, Manuel A. Ortuño, Pietro Vidossich, Enrique Gutiérrez-Puebla, Agustí Lledós,* and Salvador Conejero*

The addition of H_2 across Pt−CH_2 bonds in electron-deficient Pt(II) complexes bearing cyclometalated N-heterocyclic carbenes (NHC) leads to the corresponding 14-electron Pt(II) hydrides. The coordination of a second molecule of H_2 to form dihydrogen σ complexes strongly depends on the steric nature of the NHC ligand. The X-ray crystal structure of one of the coordinatively unsaturated Pt(II) hydrides is provided.

*A Combined **Reactivity–NMR–Computational** Study*

NHC-Governed Equilibria

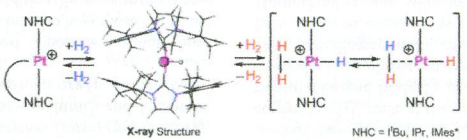

Supporting Information available via online article